Structural Engineering and Mechanics, Vol. 20, No. 6 (2005) 655-672 655
DOI: http://dx.doi.org/10.12989/sem.2005.20.6.655

Wave passage effect of seismic ground motions on the response of multiply supported structures

Y. H. Zhang† and J. H. Lin‡

State Key Laboratory of Structural Analysis for Industrial Equipment, Dalian University of Technology, Dalian, 116023, China

F. W. Williams‡† and Q. S. Li‡‡

Department of Building and Construction, City University of Hong Kong, Kowloon, Hong Kong

(Received May 26, 2004, Accepted May 17, 2005)

Abstract. Seismic random responses due to the wave passage effect are extensively investigated by using the pseudo excitation method (PEM). Two examples are used. The first is very simple but also very informative, while the second is a realistic suspension bridge. Numerical results show that the seismic responses vary significantly with wave speed, especially for low velocity or large span. Such variations are not monotonic, especially for flexible structures. The contributions of the dynamic and quasi-static components depend heavily on the seismic wave velocity and the natural frequencies of structures. For the lower natural frequency cases, the dynamic component has significant effects on the dynamic responses of the structure, whereas the quasi-static component dominates for higher natural frequencies unless the wave speed is also high. It is concluded that if insufficient data on local seismic wave velocity is available, it is advisable to select several possible velocity values in the seismic analysis and to choose the most conservative of the results thus obtained as the basis for design.

Key words: wave passage effect; earthquake; random vibration; extended structures.

1. Introduction

A rigorous seismic analysis of spatially extended structures should account for the spatial variability of the ground motion. This results from the complex nature of the earth's crust, which causes earthquake motions to vary along the length of extended structures (Harichandran and Vanmarcke 1986, Loh and Yeh 1988, Kiureghian 1996). Thus seismic responses may significantly deviate from those based on the simple assumption that the free-field ground motions are spatially uniform. Moreover, long extended structures are generally important facilities, e.g. long-span bridges, gymnasiums, dams, or nuclear power plants. Therefore, their aseismatic capabilities are

† Associate Professor, E-mail: zhangyh@dlut.edu.cn
‡ Professor, E-mail: jhlin@dlut.edu.cn
‡† Professor, Corresponding author, E-mail: williamsfw@cf.ac.uk
‡‡ Associate Professor, E-mail: bcqsli@cityu.edu.hk

highly relevant to public safety and so in the last twenty years much research has gone into establishing practical seismic analysis and design methods for them (e.g. Werner *et al.* 1979, Yamamura and Tanaka 1990, Berrah and Kausel 1992, Kiureghian and Neuenhofer 1992, Heredia-Zavoni and Vanmarcke 1994, Kiureghian and Neuenhofer 1995, Lee and Penzien 1983, Lin *et al.* 1990, Tubino *et al.* 2003, Dumanoglu and Soyluk 2003, Lin *et al.* 1992, 1997, 2004). Essentially, three basic methods have been developed, i.e., the time history method, the response spectrum method and the random vibration method.

The time history method involves solving the equations of motion directly and its chief disadvantages are that the results obtained rely heavily on the set of time histories selected and that the analysis requires extensive computational effort, which restricts the possibility of analysis with alternative sets of records (Werner *et al.* 1979).

Many researchers have instead used the random vibration method, the chief advantage of which is that it provides a statistical measure of the response which is not controlled by an arbitrary choice of the input motions (Lee and Penzien 1983, Lin *et al.* 1990, Tubino *et al.* 2003, Dumanoglu and Soyluk 2003). For example, Lee and Penzien (1983) investigated the seismic response of structures and piping systems subjected to multiple support excitations in both the time and frequency domains. Lin *et al.* (1990) simplified a surface-mounted pipeline as an infinitely long Bernoulli-Euler beam attached to evenly spaced ground supports, and solved its random seismic responses. Tubino *et al.* (2003) provided mathematical and physical interpretations of the effects of partial correlation of the seismic ground motion on the response of multi-supported multi-DOF systems by introducing suitable equivalent spectra and by representing the seismic ground motion by the proper orthogonal decomposition. Dumanoglu and Soyluk (2003) investigated the relative importance of ground motion variability effects on the dynamic behavior of a plane model of a cable-stayed bridge. However, none of these methods can deal with very complex structures due to their being relatively computationally inefficient.

To change this situation, several attempts have been made to develop an extended response spectrum method for such problems, as an approximation to the random vibration method, based on the classical response spectrum method (Yamamura and Tanaka 1990, Berrah and Kausel 1992, Kiureghian and Neuenhofer 1992, Heredia-Zavoni and Vanmarcke 1994). For computational simplicity, these methods usually ignore some important factors. For example, the support motions have been grouped into independent subgroups with perfect correlation between the members of each subgroup (Yamamura and Tanaka 1990), while alternatively, a modified spectrum method has been developed for the design of extended structures which considers the spatial variability effect arising from the incoherence alone (Berrah and Kausel 1992). A much refined method was suggested by Kiureghian and Neuenhofer (1992), but because they present the dynamic component of the response in the form of a fourfold summation, the computational effort required for complex structures is very large, especially when a large number of modes must be included in the analysis. Heredia-Zavoni and Vanmarcke (1994) reduced this formulation to a threefold summation, but the resulting precision still needs further investigation (Kiureghian and Neuenhofer 1995).

In the present paper, an efficient and strictly random vibration method, called the pseudo excitation method (PEM) (Lin *et al.* 1992, 1997, 2004), is used to investigate the influence of the wave passage effect of ground motion on the seismic responses of extended structures. In order to focus attention on the spatial variation effects, transient dynamic phenomena that may prejudice or compromise a simple interpretation of the most relevant physical and analytical aspects are ignored and the ground motion is modelled as a stationary multi-variate, one-dimensional random process.

The wave passage effect is investigated extensively in preference to the incoherence effect, because it has been shown, in most cases, to have greater influence on the seismic response of long-span cable-stayed bridges (Lin *et al.* 2004). Additionally, computation with the wave passage effect is much simpler and much more easily accepted by engineers. Therefore, in this paper we have paid more attention to the engineering application of the wave passage effect.

In the stationary random analysis of PEM, the determination of random response of a structure is converted into the determination of the response of the structure to a series of harmonic loads, i.e., so-called pseudo excitations. Advantages of this method are that less computation effort is required and that the cross-correlations both between normal modes and between excitations are automatically included. The theory used is not original to this paper, but it is relatively new and so for completeness of the paper it is summarised with adequate detail in the next two sections. The results then follow. They are original and are used to draw many general and useful conclusions. The first set of results presented is for the internal forces of a single-degree-of-freedom system with two elastic supports and consists of the expected maximum response values for different apparent wave velocities and natural frequencies, with the latter progressively altered by changing the elastic support stiffness. In addition, the relative importance of the influences of the quasi-static and dynamic response components is discussed. Then, a realistic long-span suspension bridge is analyzed with different apparent wave velocities, to enable the influence of the wave passage effect to be further discussed.

2. Model of random field considering wave passage effect

The seismic ground motion is assumed to be a normal stationary random process. If a structure has N supports, the cross power spectral density function of the ground accelerations $\ddot{u}_k(t)$ and $\ddot{u}_l(t)$ at the kth and lth supports can be written as

$$S_{kl}(\omega) = \gamma_{kl}(\omega)\sqrt{S_{kk}(\omega)S_{ll}(\omega)} \tag{1}$$

in which: ω is the circular frequency;

$$\gamma_{kl}(i\omega) = \rho_{kl}(i\omega)\exp[i\theta_{kl}(\omega)], \quad \rho_{kl}(i\omega) \le 1 \tag{2}$$

is the coherency function of the accelerations at the kth and lth supports; $S_{kk}(\omega)$ and $S_{ll}(\omega)$ are the power spectral density functions of the accelerations at the kth and lth supports, which represent the local effect, and; $\exp[i\theta_{kl}(\omega)]$ represents the wave passage effect (neglecting the local site effect), which can be written as

$$\exp[i\theta_{kl}(\omega)] = \exp[-i\omega d_{kl}^L/v_{app}] \tag{3}$$

Here: d_{kl}^L is the projection in the earthquake propagation direction of the distance d_{kl} between the two supports, and; v_{app} is the apparent earthquake wave velocity. Suppose that the wave front reaches the origin of the coordinate system, i.e., the reference point, at $T = 0$, and then reaches the ground joints at times T_1, T_2, …, T_N, respectively. Without losing generality, we can assume $T_l \ge T_k$, thus

$$d_{kl}^L/v_{app} = T_l - T_k \tag{4}$$

and

$$\exp[-i\omega d_{kl}^L/v_{app}] = \exp[i\omega(T_k - T_l)] \tag{5}$$

The ground motion accelerations of all the supports can be written as the N dimensional vector (where superscript T denotes transpose)

$$\ddot{\boldsymbol{u}}_b(t) = \{\ddot{u}_1(t) \ \ \ddot{u}_2(t) \ \ldots \ \ddot{u}_N(t)\}^T \tag{6}$$

and their statistical characteristics can be expressed by the power spectral density matrix

$$\boldsymbol{S}_{\ddot{u}_b\ddot{u}_b}(\omega) = \begin{bmatrix} S_{11}(\omega) & S_{12}(\omega) & \ldots & S_{1N}(\omega) \\ S_{21}(\omega) & S_{22}(\omega) & \ldots & S_{2N}(\omega) \\ \vdots & \vdots & \ddots & \vdots \\ S_{N1}(\omega) & S_{N2}(\omega) & \ldots & S_{NN}(\omega) \end{bmatrix} \tag{7}$$

When only the wave passage effect is considered, $\rho_{kl}(i\omega) \equiv 1$, and $S_{kk}(\omega) = S_{ll}(\omega) = S_b(\omega)$. Thus, Eq. (7) can be written as (where superscript * denotes conjugate)

$$\boldsymbol{S}_{\ddot{u}_b\ddot{u}_b}(\omega) = \begin{bmatrix} 1 & e^{i\omega(T_1-T_2)} & \ldots & e^{i\omega(T_1-T_N)} \\ e^{i\omega(T_2-T_1)} & 1 & \ldots & e^{i\omega(T_2-T_N)} \\ \vdots & \vdots & \ddots & \vdots \\ e^{i\omega(T_N-T_1)} & e^{i\omega(T_N-T_2)} & \ldots & 1 \end{bmatrix} S_b(\omega) = S_b(\omega)\boldsymbol{e}^*\boldsymbol{e}^T \tag{8}$$

in which

$$\boldsymbol{e} = \{e^{-i\omega T_1} \ \ e^{-i\omega T_2} \ \ldots \ e^{-i\omega T_N}\}^T \tag{9}$$

3. Pseudo excitation method considering wave passage effect

For the structure with N supports, the equations of motion can be written in the matrix form

$$\begin{bmatrix} \boldsymbol{M} & \boldsymbol{M}_C \\ \boldsymbol{M}_C^T & \boldsymbol{M}_G \end{bmatrix}\begin{bmatrix} \ddot{\boldsymbol{u}} \\ \ddot{\boldsymbol{u}}_G \end{bmatrix} + \begin{bmatrix} \boldsymbol{C} & \boldsymbol{C}_C \\ \boldsymbol{C}_C^T & \boldsymbol{C}_G \end{bmatrix}\begin{bmatrix} \dot{\boldsymbol{u}} \\ \dot{\boldsymbol{u}}_G \end{bmatrix} + \begin{bmatrix} \boldsymbol{K} & \boldsymbol{K}_C \\ \boldsymbol{K}_C^T & \boldsymbol{K}_G \end{bmatrix}\begin{bmatrix} \boldsymbol{u} \\ \boldsymbol{u}_G \end{bmatrix} = \begin{Bmatrix} 0 \\ \boldsymbol{F}_G \end{Bmatrix} \tag{10}$$

in which: $\boldsymbol{u}_G$ is the m-dimensional vector of enforced support displacement components, e.g., so that $m = 3N$; $\boldsymbol{u}$ is an n-dimensional vector containing all nodal displacements except those at the supports; $\boldsymbol{F}_G$ represents the enforced forces at all supports; the $n \times n$ matrices $\boldsymbol{M}$, $\boldsymbol{C}$ and $\boldsymbol{K}$ are respectively the mass, damping and stiffness matrices associated with $\boldsymbol{u}$; the $m \times m$ matrices $\boldsymbol{M}_G$, $\boldsymbol{C}_G$ and $\boldsymbol{K}_G$ are the mass, damping and stiffness matrices associated with $\boldsymbol{u}_G$ and; $\boldsymbol{M}_C$, $\boldsymbol{C}_C$ and $\boldsymbol{K}_C$ are the $n \times m$ coupling matrices shown. Note that when the lumped mass matrix approximation is adopted, $\boldsymbol{M}_C$ is null. In order to solve Eq. (10), $\boldsymbol{u}$ is decomposed into the two parts

$$\boldsymbol{u} = \boldsymbol{u}^s + \boldsymbol{u}^d \tag{11}$$

where $\boldsymbol{u}^s$ and $\boldsymbol{u}^d$ are respectively the quasi-static and dynamic displacement vectors, which satisfy the equations

$$\boldsymbol{u}^s = -\boldsymbol{K}^{-1}\boldsymbol{K}_C\boldsymbol{u}_G \equiv \boldsymbol{R}\boldsymbol{u}_G \tag{12}$$

$$\boldsymbol{M}\ddot{\boldsymbol{u}}^d + \boldsymbol{C}\dot{\boldsymbol{u}}^d + \boldsymbol{K}\boldsymbol{u}^d = -(\boldsymbol{M}\boldsymbol{R} + \boldsymbol{M}_C)\ddot{\boldsymbol{u}}_G \tag{13}$$

Seismic waves can be divided into body waves and surface waves. Body waves include the longitudinal waves (alternatively called the pressure, primary or P waves) and the transverse waves, which are alternatively called the shear, secondary or S waves. Surface waves include Rayleigh waves and Love waves. For P waves, the soil particles move parallel to the travelling direction of waves, whereas for S waves they move normal to this direction. For horizontal shear waves i.e., SH waves, all particles move horizontally and for vertical shear waves, i.e., SV waves, they all move vertically.

Assume that xyz is a right-hand co-ordinate system for which both the x and y axes lie in the horizontal plane. The anti-clockwise angle between the x axis and the horizontal travelling direction of waves is β. Thus, the acceleration components along the coordinate axes, $\ddot{\boldsymbol{u}}_G$, can be expressed in terms of the components parallel or normal to the wave traveling direction, $\ddot{\boldsymbol{u}}_b$, as

$$\ddot{\boldsymbol{u}}_G = \boldsymbol{E}_{mN}\ddot{\boldsymbol{u}}_b \tag{14}$$

in which $\boldsymbol{E}_{mN}$ is an $m \times N$ block-diagonal matrix.

$$\boldsymbol{E}_{mN} = \mathrm{diag}[\boldsymbol{E}_1 \;\; \boldsymbol{E}_2 \;\; \ldots \;\; \boldsymbol{E}_N] \tag{15}$$

Hence when all three translations and no rotational components are considered for each support, $m = 3N$ and each sub-matrix $\boldsymbol{E}_i$ becomes $[\cos\beta \;\; \sin\beta \;\; 0]^T$, $[-\sin\beta \;\; \cos\beta \;\; 0]^T$ and $[0 \;\; 0 \;\; 1]^T$ for the P, SH and SV waves, respectively.

Using Eq. (14), Eqs. (12) and (13) can be rewritten as

$$\boldsymbol{u}^s = -\boldsymbol{K}^{-1}\boldsymbol{K}_C\boldsymbol{u}_G \equiv \boldsymbol{R}\boldsymbol{E}_{mN}\boldsymbol{u}_b \tag{16}$$

$$\boldsymbol{M}\ddot{\boldsymbol{u}}^d + \boldsymbol{C}\dot{\boldsymbol{u}}^d + \boldsymbol{K}\boldsymbol{u}^d = -(\boldsymbol{M}\boldsymbol{R} + \boldsymbol{M}_C)\boldsymbol{E}_{mN}\ddot{\boldsymbol{u}}_b \tag{17}$$

Let any general response quantities of interest be denoted by $z(t)$, which could therefore be a nodal displacement vector, an internal force vector, a stress vector or a strain vector. Then for a linear system $z(t)$ can be expressed as a linear function of the nodal and support displacements, i.e.,

$$z(t) = \boldsymbol{T}^T\boldsymbol{u}(t) + \boldsymbol{T}_G^T\boldsymbol{u}_G(t) \tag{18}$$

where $\boldsymbol{T}^T$ and $\boldsymbol{T}_G^T$ are transfer matrices which usually depend on the geometry and stiffness properties of the structural system. The dynamic displacement vector can then be written in the convolution integral form

$$\boldsymbol{u}^d(t) = -\int_{-\infty}^{\infty} \boldsymbol{h}(\tau)(\boldsymbol{MR} + \boldsymbol{M}_C)\boldsymbol{E}_{mN}\ddot{\boldsymbol{u}}_b(t-\tau)d\tau \tag{19}$$

in which, $\boldsymbol{h}(\tau)$ is the impulse response function matrix. Thus, using Eqs. (14), (16) and (19), Eq. (18) becomes

$$\boldsymbol{z}(t) = -\boldsymbol{T}^T\int_{-\infty}^{\infty} \boldsymbol{h}(\tau)(\boldsymbol{MR} + \boldsymbol{M}_C)\boldsymbol{E}_{mN}\ddot{\boldsymbol{u}}_b(t-\tau)d\tau + (\boldsymbol{T}^T\boldsymbol{RE}_{mN} + \boldsymbol{T}_G^T\boldsymbol{E}_{mN})\boldsymbol{u}_b(t) \tag{20}$$

Then the power spectrum density matrix of $\boldsymbol{z}(t)$ can be obtained as

$$\begin{aligned} \boldsymbol{S}_{zz}(\omega) &= \boldsymbol{T}^T\boldsymbol{H}^*(\omega)(\boldsymbol{MR} + \boldsymbol{M}_C)\boldsymbol{E}_{mN}\boldsymbol{S}_{\ddot{u}_b\ddot{u}_b}(\omega)\boldsymbol{E}_{mN}^T(\boldsymbol{MR} + \boldsymbol{M}_C)^T\boldsymbol{H}^T(\omega)\boldsymbol{T} \\ &+ \frac{1}{\omega^2}\boldsymbol{T}^T\boldsymbol{H}^*(\omega)(\boldsymbol{MR} + \boldsymbol{M}_C)\boldsymbol{E}_{mN}\boldsymbol{S}_{\ddot{u}_b\ddot{u}_b}(\omega)(\boldsymbol{E}_{mN}^T\boldsymbol{R}^T\boldsymbol{T} + \boldsymbol{E}_{mN}^T\boldsymbol{T}_G) \\ &+ \frac{1}{\omega^2}(\boldsymbol{T}^T\boldsymbol{RE}_{mN} + \boldsymbol{T}_G^T\boldsymbol{E}_{mN})\boldsymbol{S}_{\ddot{u}_b\ddot{u}_b}(\omega)\boldsymbol{E}_{mN}^T(\boldsymbol{MR} + \boldsymbol{M}_C)^T\boldsymbol{H}^T(\omega)\boldsymbol{T} \\ &+ \frac{1}{\omega^4}(\boldsymbol{T}^T\boldsymbol{RE}_{mN} + \boldsymbol{T}_G^T\boldsymbol{E}_{mN})\boldsymbol{S}_{\ddot{u}_b\ddot{u}_b}(\omega)(\boldsymbol{E}_{mN}^T\boldsymbol{R}^T\boldsymbol{T} + \boldsymbol{E}_{mN}^T\boldsymbol{T}_G) \\ &= \left(\boldsymbol{T}^T\boldsymbol{H}(\omega)(\boldsymbol{MR} + \boldsymbol{M}_C)\boldsymbol{E}_{mN} + \frac{\boldsymbol{T}^T\boldsymbol{RE}_{mN} + \boldsymbol{T}_G^T\boldsymbol{E}_{mN}}{\omega^2}\right)^*\boldsymbol{S}_{\ddot{u}_b\ddot{u}_b}(\omega) \\ &\quad \left(\boldsymbol{T}^T\boldsymbol{H}(\omega)(\boldsymbol{MR} + \boldsymbol{M}_C)\boldsymbol{E}_{mN} + \frac{\boldsymbol{T}^T\boldsymbol{RE}_{mN} + \boldsymbol{T}_G^T\boldsymbol{E}_{mN}}{\omega^2}\right)^T \end{aligned} \tag{21}$$

in which $\boldsymbol{H}(\omega)$ is the frequency response function matrix of the structure and is given by

$$\boldsymbol{H}(\omega) = \int_{-\infty}^{\infty} \boldsymbol{h}(t)e^{-i\omega\tau}d\tau \tag{22}$$

The four terms summed to give the first equality of Eq. (21) can be grouped into three parts. These are: the first term corresponds to the contribution of the dynamic component; the fourth term corresponds the contribution of the quasi-static component and; the sum of the second and the third terms represents the contribution of their cross-correlation.

Substituting Eq. (8) into Eq. (21), the power spectrum density matrix of $\boldsymbol{z}(t)$ is expressed by

$$\boldsymbol{S}_{zz}(\omega) = \boldsymbol{p}^*\boldsymbol{p}^T \tag{23}$$

where

$$\boldsymbol{p} = \left(\boldsymbol{T}^T\boldsymbol{H}(\omega)(\boldsymbol{MR} + \boldsymbol{M}_C)\boldsymbol{E}_{mN} + \frac{\boldsymbol{T}^T\boldsymbol{RE}_{mN} + \boldsymbol{T}_G^T\boldsymbol{E}_{mN}}{\omega^2}\right)\sqrt{S_b(\omega)}\boldsymbol{e} \tag{24}$$

Based on PEM, the pseudo excitation vector can be constructed as

$$\tilde{\ddot{\boldsymbol{u}}}_b = \sqrt{S_b(\omega)}\boldsymbol{e}\exp(i\omega t) \tag{25}$$

after which solving the deterministic equation

$$\boldsymbol{M}\ddot{\tilde{\boldsymbol{u}}}^d + \boldsymbol{C}\dot{\tilde{\boldsymbol{u}}}^d + \boldsymbol{K}\tilde{\boldsymbol{u}}^d = -(\boldsymbol{MR} + \boldsymbol{M}_C)\boldsymbol{E}_{mN}\ddot{\tilde{\boldsymbol{u}}}_b \tag{26}$$

gives the pseudo dynamic displacement vector $\tilde{\boldsymbol{u}}^d$ as

$$\tilde{\boldsymbol{u}}^d = -\boldsymbol{H}(\omega)(\boldsymbol{MR} + \boldsymbol{M}_C)\boldsymbol{E}_{mN}\sqrt{S_b(\omega)}\boldsymbol{e}\exp(i\omega t) \tag{27}$$

Then, the pseudo quasi-static displacement vector is easily obtained by solving the linear algebraic equation

$$\boldsymbol{K}\tilde{\boldsymbol{u}}^s = \frac{1}{\omega^2}\boldsymbol{K}_C\boldsymbol{E}_{mN}\ddot{\tilde{\boldsymbol{u}}}_b \tag{28}$$

which can be written in the form

$$\tilde{\boldsymbol{u}}^s = -\frac{1}{\omega^2}\boldsymbol{RE}_{mN}\sqrt{S_b(\omega)}\boldsymbol{e}\exp(i\omega t) \tag{29}$$

and the pseudo displacement components of support motion along the coordinate axes

$$\tilde{\boldsymbol{u}}_G = -\frac{1}{\omega^2}\boldsymbol{E}_{mN}\sqrt{S_b(\omega)}\boldsymbol{e}\exp(i\omega t) \tag{30}$$

Therefore, the pseudo response $\tilde{z}(t)$ can be expressed as

$$\tilde{z}(t) = -\left(\boldsymbol{T}^T\boldsymbol{H}(\omega)(\boldsymbol{MR} + \boldsymbol{M}_C)\boldsymbol{E}_{mN} + \frac{\boldsymbol{T}^T\boldsymbol{RE}_{mN} + \boldsymbol{T}_G^T\boldsymbol{E}_{mN}}{\omega^2}\right)\sqrt{S_b(\omega)}\boldsymbol{e}\exp(i\omega t) \tag{31}$$

Comparing Eq. (31) with Eqs. (23) and (24), it is not difficult to obtain the relationship

$$\boldsymbol{S}_{zz}(\omega) = z^*(t)\boldsymbol{z}^T(t) \tag{32}$$

The required spectral moments of the responses can then be obtained, and so the extreme values can be estimated (Davenport 1961).

The above has summarised the key details of pseudo excitation method associated with multi-support seismic analysis, i.e., the method used to obtain the results which follow. It is clear that no approximation has been introduced into the derivation of the pseudo excitation method in order to compute various kinds of power spectrum density functions. Because the harmonic analysis function is available in almost all FEM programs, it is very simple to compute the auto- and cross-PSDs, e.g. for displacements, internal forces and strains, etc.

4. Numerical examples

Two examples are presented. The first one is very simple and is used because it enables wide ranging general conclusions to be drawn with minimum demands on the reader. It also allows the natural frequencies to be altered very easily, which cannot be done so easily for more realistic

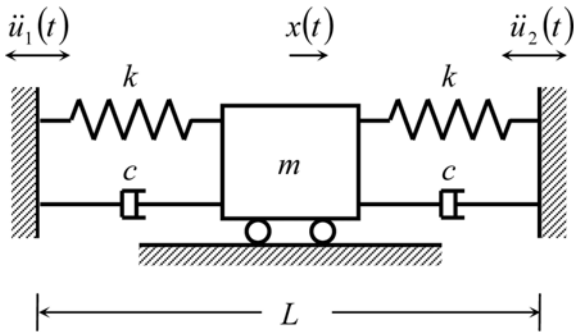

Fig. 1 A single degree of freedom system with two support excitations

problems. The second example is a realistic problem and shows the power of the PEM method used as well as leading to further general conclusions.

Example 1 A single degree of freedom system with support excitations at each end is shown in Fig. 1. The mass is m, the stiffness is k, the damping coefficient is c and the distance between the two supports is L. The seismic wave motion is in the direction of the x axis and its velocity is v.

Firstly, the power spectral density of the internal force of the left-hand spring is derived analytically by PEM, giving

$$S_{N_1} = S_{N_1}^r + S_{N_1}^s + S_{N_1}^{rs} \tag{33}$$

where

$$S_{N_1}^r(\omega) = \frac{0.5k^2 S_b(\omega)}{(\omega_0^2 - \omega^2)^2 + 4\xi^2\omega_0^2\omega^2}(1 + \cos\omega T) \tag{34}$$

$$S_{N_1}^s(\omega) = -\frac{0.5k^2 S_b(\omega)}{\omega^4}(1 - \cos\omega T) \tag{35}$$

$$S_{N_1}^{rs}(\omega) = \frac{2k^2 S_b(\omega)\xi\omega_0/\omega}{(\omega_0^2 - \omega^2)^2 + 4\xi^2\omega_0^2\omega^2}\sin\omega T \tag{36}$$

represent, respectively, the contributions of the dynamic displacements, the quasi-static displacements and the contribution of their coupling. Here: $\omega_0 = \sqrt{2k/m}$; $\xi = c/m\omega_0$ and; $T = L/v$. In the computation that follows, $m = 1.0$, $\xi = 0.05$, and the Penzien spectrum

$$S_b(\omega) = \frac{1 + 4\xi_g^2(\omega/\omega_g)^2}{[1 - (\omega/\omega_g)^2]^2 + 4\xi_g^2(\omega/\omega_g)^2}\frac{\omega^4}{(\omega^2 - \omega_f^2)^2 + 4\omega^2\omega_f^2\xi_f^2}S_0 \tag{37}$$

is used (Clough and Penzien 1993). The spectrum parameters used were: $\omega_g = 15.0$ rad/s; $\xi_g = 0.6$; $\omega_f = 1.5$ rad/s; $\xi_f = 0.6$ and; $S_0 = 0.00177$ m^2s^{-3} (Dumanoglu and Soyluk 2003).

Given the power spectral density functions, the internal force spectral moments of the left-hand spring, N_1, and its extreme can be easily computed (Davenport 1961). Let $\overline{N}_1$ be the expected

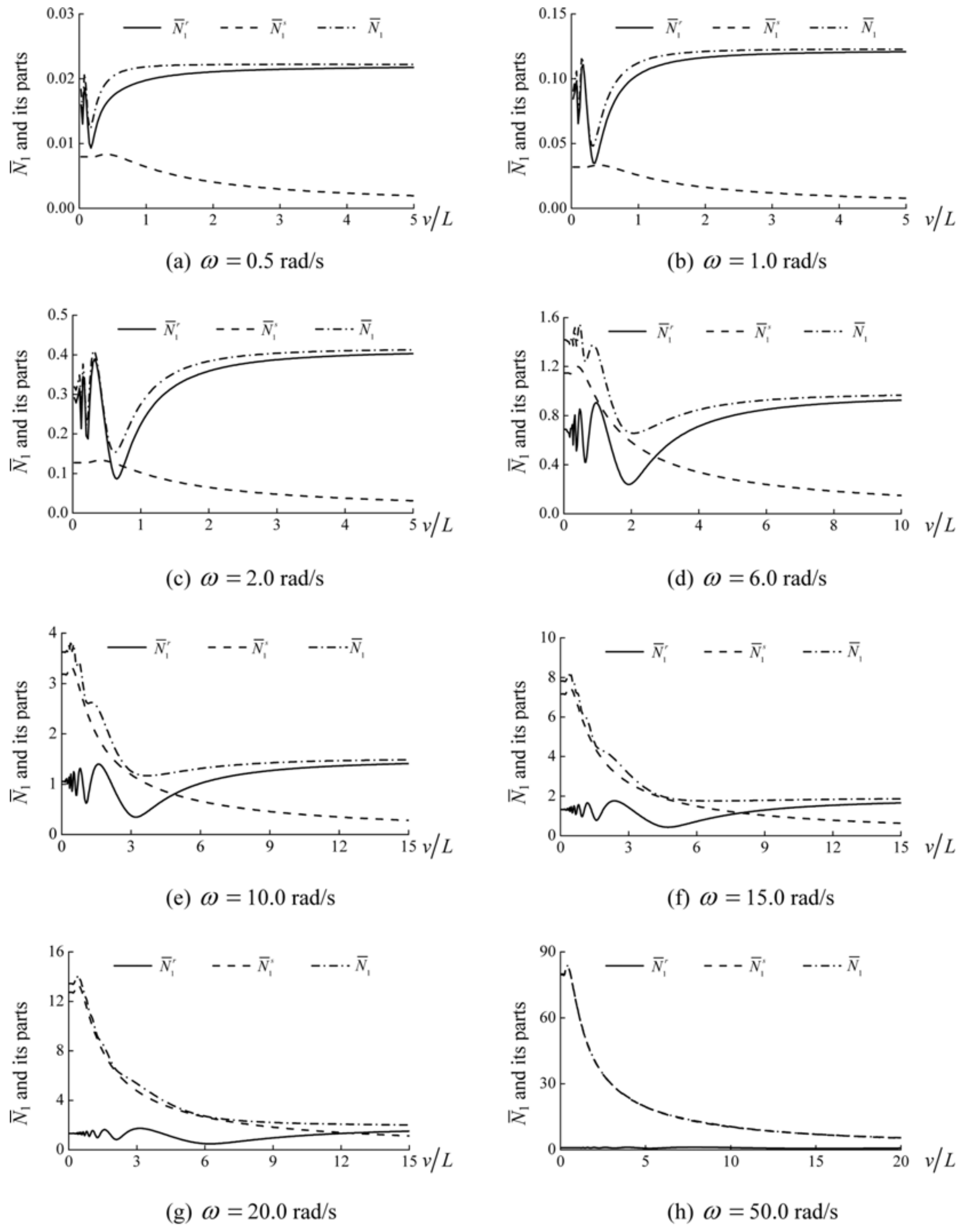

Fig. 2 Variations of internal forces with wave speed for different natural angular frequencies ω

extreme value of N_1, which consists of the three parts, $\overline{N}_1^r$, $\overline{N}_1^s$ and $\overline{N}_1^{rs}$, which respectively represent the contribution of the dynamic displacements, the quasi-static displacements and their coupling. Different values of the stiffness of the two springs were adopted to investigate the wave passage effect. This gave the variation of $\overline{N}_1$, $\overline{N}_1^r$ and $\overline{N}_1^s$ with velocity, or v/L, shown in Fig. 2. (The contribution of the coupling part, $\overline{N}_1^{rs}$, is very small compared with the contributions of $\overline{N}_1^r$ and $\overline{N}_1^s$ and so for clarity it is not given in Fig. 2, because it can be deduced as $\overline{N}_1 - \overline{N}_1^r - \overline{N}_1^s$.)

It can be seen that:

(1) The seismic responses vary significantly with wave speed, especially when v/L is very small, i.e., for low velocity or large span. In general, these results and those for more complex problems, e.g. Example 2 below, show that such variations are not monotonic, especially for flexible structures.

(2) The contributions of the dynamic and quasi-static components depend heavily on the seismic wave velocity and the natural frequencies of structures. For the lower natural frequencies, i.e., more flexible structures, the dynamic component has significant effects on the dynamic responses of the structure, whereas the quasi-static component dominates for higher natural frequencies unless the wave speed is also high.

(3) For large values of v/L, $\overline{N}_1^r$ increases monotonically as v/L increases, while $\overline{N}_1^s$ decreases monotonically and approaches zero as $v/L \to \infty$.

(4) When the system's natural frequency is small, i.e., the structure is flexible, the internal force responses obtained by neglecting the wave passage effect (i.e., by assuming $v/L \to \infty$) err on the safe side, but for the cases with larger natural frequencies they give extremely unsafe predictions of the response for low wave speeds.

Example 2 Consider the suspension bridge shown in Fig. 3, which is 330 m long, 26.5 m wide, has a main span of length 160 m and towers of height 42 m. Although small, this bridge is similar to one recently built on a sensitive site because of its architectural merit. The finite element model used had: 369 nodes, including 12 support ones; 484 elements and; 972 degrees of freedom. As

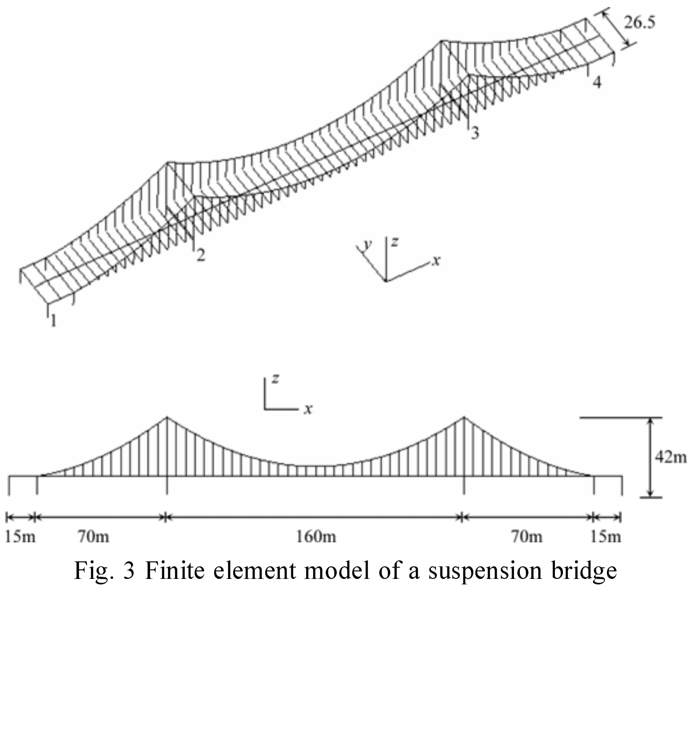

Fig. 3 Finite element model of a suspension bridge

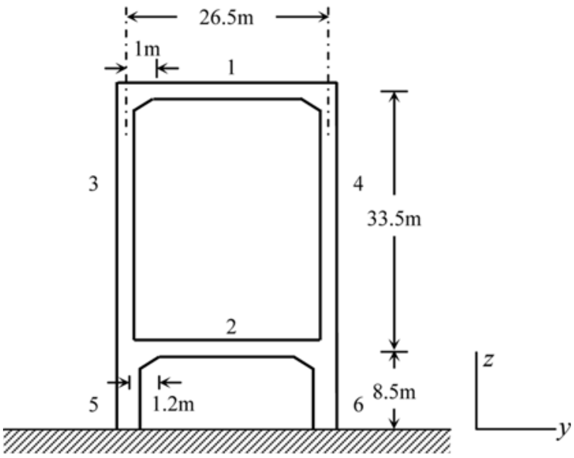

Fig. 4 Configuration of the tower. The deck rests on beam 2.

Fig. 3 indicates, the bridge deck was modelled as a three-dimensional beam with appropriate rigidities and with rigid arms which connected it to the bottoms of the hangers. Timoshenko theory was used for this beam. Three-dimensional Timoshenko beam elements were also used to model the two columns and both beams of each bridge tower, see Fig. 4, but with rigid arms of length 1 m used to represent the haunches at the ends of the beams. The geometric nonlinearity due to the large deformation of the cables was allowed for when determining the initial shape of the bridge and three-dimensional taut string theory for extensible straight members was used to model both the hangers and the cable portions between the attachment points of adjacent hangers. The total masses of the deck, towers, piers, cables and hangers were, respectively, 2.17×10^7, 4.532×10^6, 6.874×10^6, 1.464×10^6 and 1.075×10^5 kg. Other properties of the model are listed in Table 1.

Table 1 Properties of the model of the suspension bridge

Member		EI_i (Nm^2)	EI_o (Nm^2)	GJ (Nm^2)	EA (N)	μ (kg/m)
tower	1	1.71×10^{11}	1.79×10^{11}	2.26×10^{10}	1.73×10^{11}	12375.0
	2	1.71×10^{11}	1.79×10^{11}	2.26×10^{10}	1.73×10^{11}	12375.0
	3	1.14×10^{11}	1.14×10^{11}	8.24×10^{10}	2.19×10^{11}	15625.0
	4	1.14×10^{11}	1.14×10^{11}	8.24×10^{10}	2.19×10^{11}	15625.0
	5	4.38×10^{11}	4.38×10^{11}	3.40×10^{11}	4.29×10^{11}	30625.0
	6	4.38×10^{11}	4.38×10^{11}	3.40×10^{11}	4.29×10^{11}	30625.0
deck		4.81×10^{10}	1.31×10^{13}	8.25×10^{10}	5.78×10^{11}	41250.0
cables		-	-	-	2.826×10^{10}	2241.2
hangers		-	-	-	1.769×10^9	73.1

Key: EI_i = rigidity for flexure in the xz(yz) plane of the deck (tower);
EI_o = rigidity for flexure in the plane perpendicular to that of EI_i;
GJ = torsional rigidity;
EA = extensional rigidity and;
μ = mass per unit length

Table 2 The first 15 natural frequencies (in rad/s) and mode shapes of the suspension bridge

Mode	Frequency	Type	n_h	Mode	Frequency	Type	n_h
1	4.234	V	1p	9	12.157	T	2p
2	5.860	V	2p	10	14.360	V	4t
3	7.994	V	3p	11	14.419	L	6p
4	8.644	V	4p	12	14.992	V	7p
5	8.811	T	1p	13	15.296	H	2t
6	9.180	V	5p	14	15.392	H	3t
7	9.876	H	1t	15	15.916	L	8p
8	11.178	V	3t				

Key: V = vertical mode, with deck and cables moving in phase;
T = torsional mode, i.e., deck twists and cables move vertically but out of phase;
H = sway mode, with deck and cables moving in phase;
L = longitudinal mode, with considerable out-of-plane tower flexure;
n_h = number of half waves mode has between the piers (p) or towers (t)

The first 50 modes were used in the mode superposition analysis and Table 2 lists the first 15 natural frequencies and gives an indication of their mode shapes. Hence the circular frequencies of the bridge were 4.234 rad/s (i.e., the basic period was 1.48 s) for the fundamental vertical mode, 8.811 rad/s for the fundamental torsional mode and 9.876 rad/s for the fundamental horizontal mode.

The seismic spatial effects for P waves, SH waves and SV waves travelling in the longitudinal direction of the bridge were investigated and the critical damping ratio was assumed to be 0.02 for each mode. The Penzien spectrum model was again adopted and the values used for the parameters were identical to those used in Example 1. The seismic analysis was executed for 53 apparent wave speeds ranging from 300 to 6000 m/s. This range was chosen to give added interest to the results by covering a wide spectrum of apparent wave speeds, although this bridge has relatively stiff soil for which the range 1,000-5,000 m/s is most relevant. Figs. 5 and 6 give the shear forces and moments obtained at supports 1, 2, 3 and 4 of Fig. 3. Supports 1, 2, 3, and 4 were chosen because, for P waves, they are the most critical part of the bridge. It can be seen that the wave velocities have significant influence on the seismic responses, especially for lower wave velocities. When the wave speed is low, e.g. 300 m/s, the seismic internal forces may exceed twice those due to uniform ground motion, which corresponds to infinite wave speed. It can also be seen from Figs. 5 and 6 that the bridge responses might decrease or increase depending on the location of the structural points and the response quantity of interest. This point of view is identical to that obtained by Hawwari (1992) in a study of a more flexible suspension bridge model. Moreover, the shear forces and moments at the four supports obtained by neglecting the wave passage effect may give extremely unsafe predictions of the response, though the bridge is flexible (the fundamental natural frequency is 4.234 rad/s). This seems inconsistent with point 4 of Example 1. The reason is that the fundamental natural frequency is usually not the only main participating natural frequency that will affect the structural responses severely. This can be seen from the corresponding PSD curves described below.

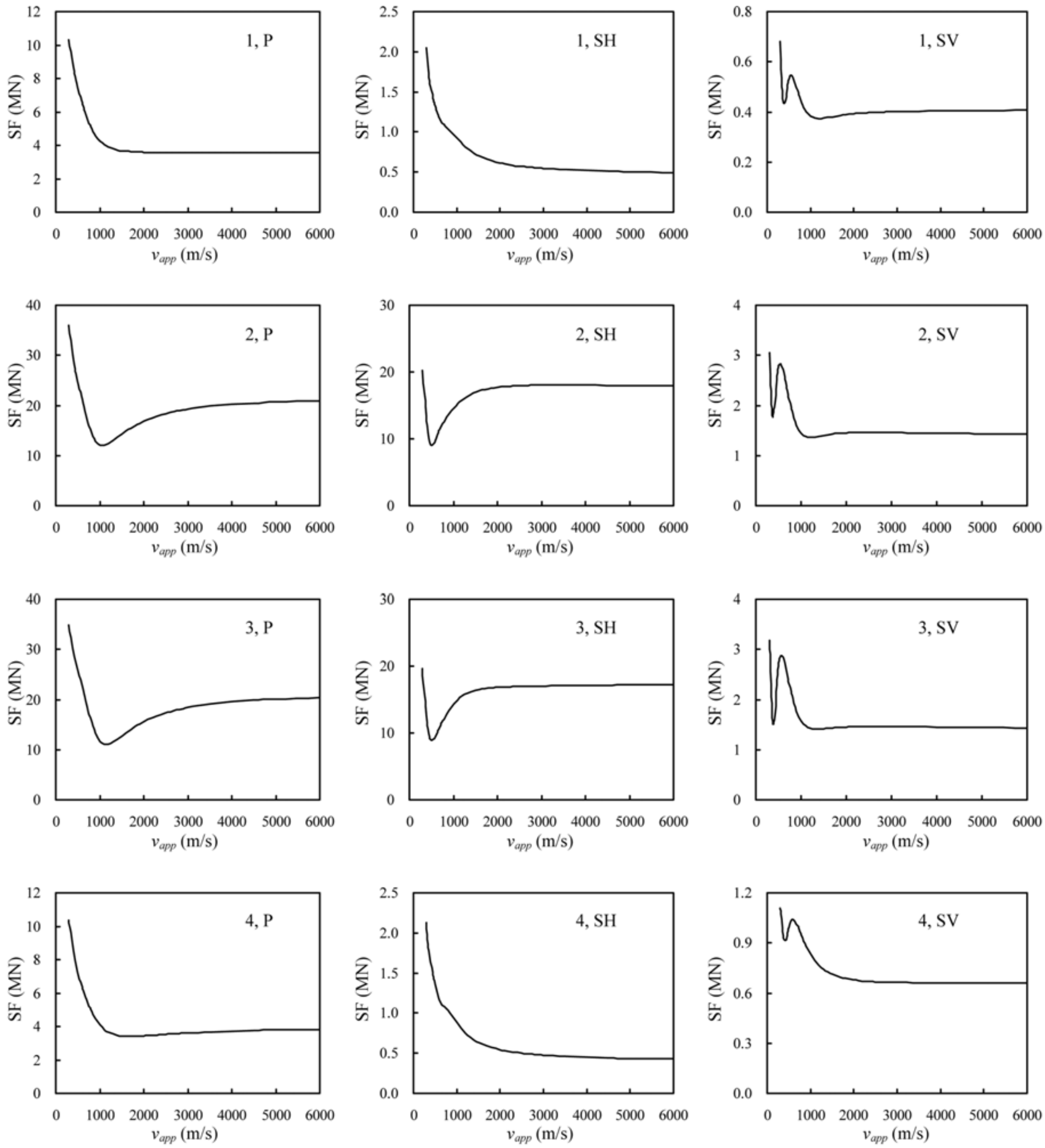

Fig. 5 Variation of the shear forces at supports 1-4 due to different wave velocities. The support number and wave type are shown within each graph, for which the vertical axis gives the shear force (SF) and the horizontal axis gives the wave velocity.

For a P wave, the PSD curves of the shear force at support 2 in the x direction are shown in Fig. 7(a), and the corresponding PSD curves of the bending moment in the xz plane are shown in Fig. 7(b). Clearly, when the wave velocity is infinite, the PSD curves have two peaks near 14.419

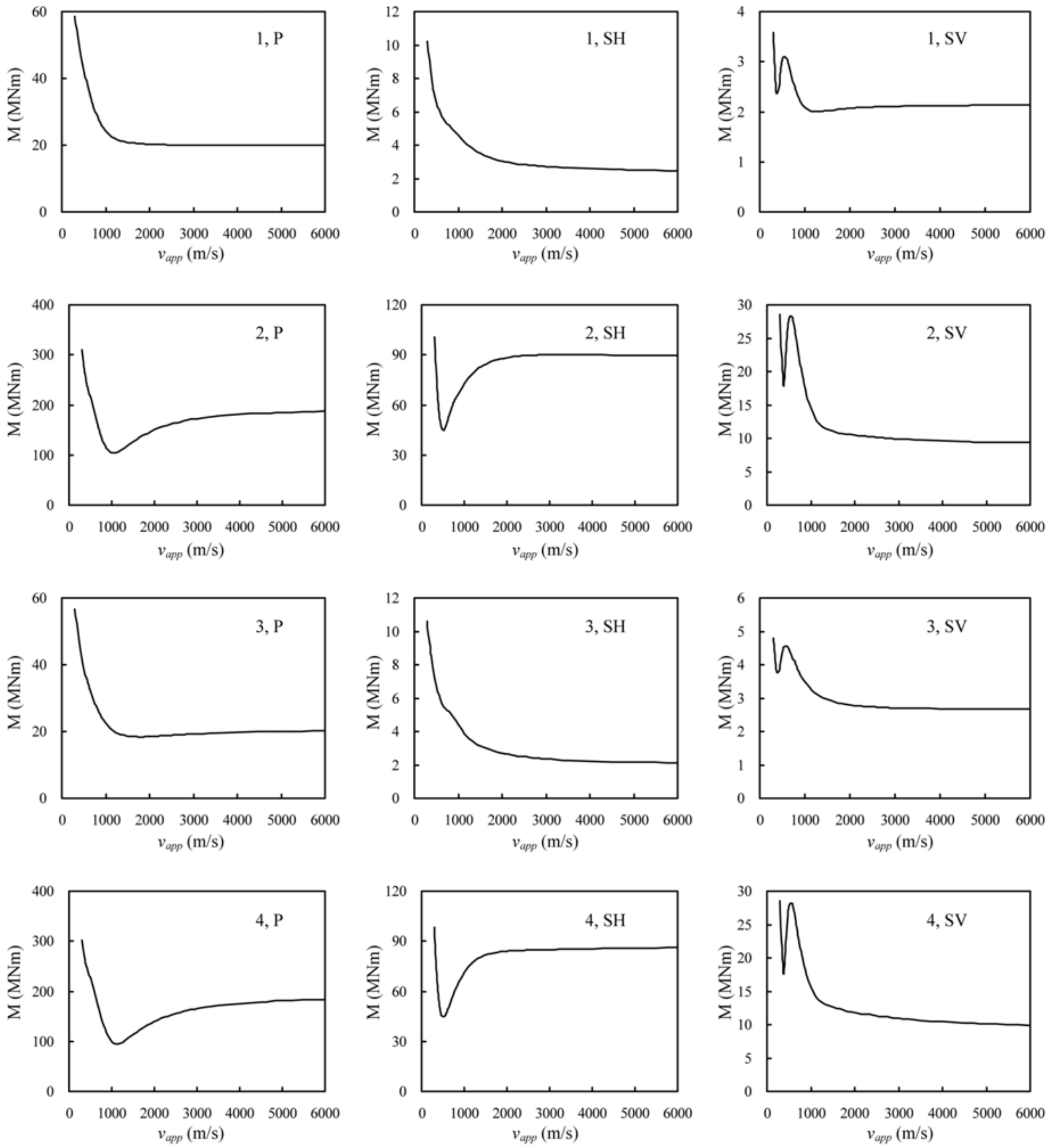

Fig. 6 Variation of the moments at supports 1-4 due to different wave velocities. The support number and wave type are shown within each graph, for which the vertical axis gives the moment (M) and the horizontal axis gives the wave velocity.

rad/s and 15.916 rad/s, which are the first and the second longitudinal natural frequencies of the structure. For the wave velocity of 1000 m/s, there is also an additional peak at about 1.5 rad/s, which is the first filter frequency ω_f of the ground motion and is much lower than the fundamental frequency of the bridge. This peak reflects the influence of quasi-static displacements. Thus it can be seen that at the lower wave velocity of 500 m/s the amplitudes of these three peaks varied very considerably, which reflects similar influences of wave speed on the dynamic and quasi-static displacements as those observed above for Example 1. It is to be expected that the PSD plots corresponding to SH and SV waves would have peaks close to, respectively, the H and V modes of Table 2, i.e., close to 9.876 rad/s for the SH waves and, for the SV waves, close to 4.234, 5.860, 7.994, 8.644, 9.180, 11.178, 14.360 and 14.992 rad/s. Fig. 8 confirms this prediction. However, in these two cases, the contributions of quasi-static displacements are not as significant as those in Fig. 7.

When designing a complex structure, it is usually difficult to judge the main participating natural frequencies that will affect the structural responses severely. Moreover, the seismic wave velocity may vary significantly with different circumstances. Therefore, for practical designs, if data on the local seismic wave velocity is unavailable or insufficient, it is advisable to select several possible velocity values in the seismic analysis and then to use the most conservative results for design. This can be done very conveniently when using PEM.

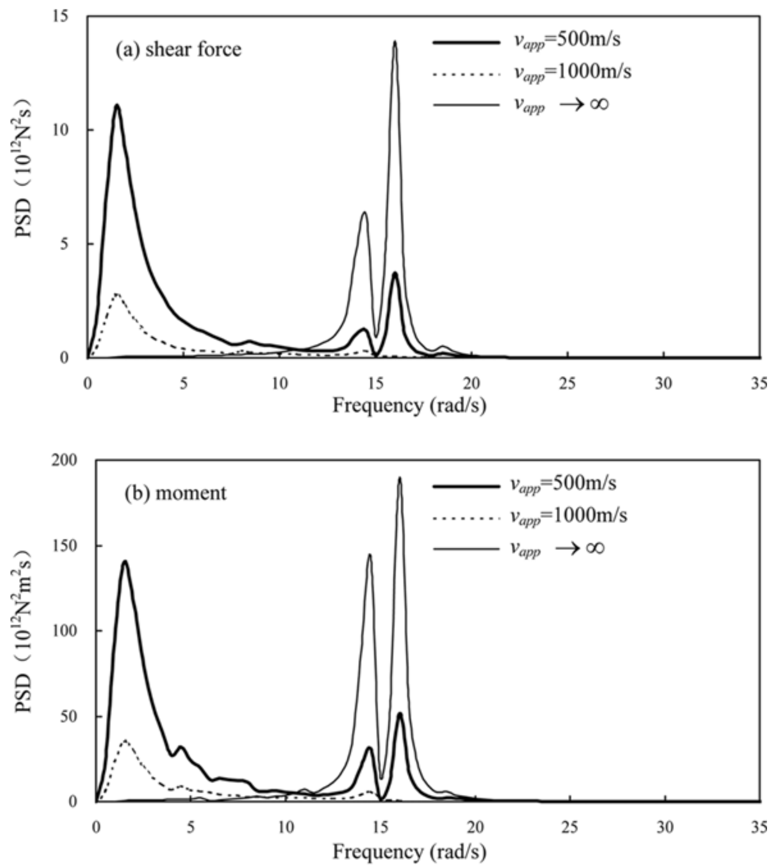

Fig. 7 Power spectral density of the shear force and moment at support 2 due to a P wave

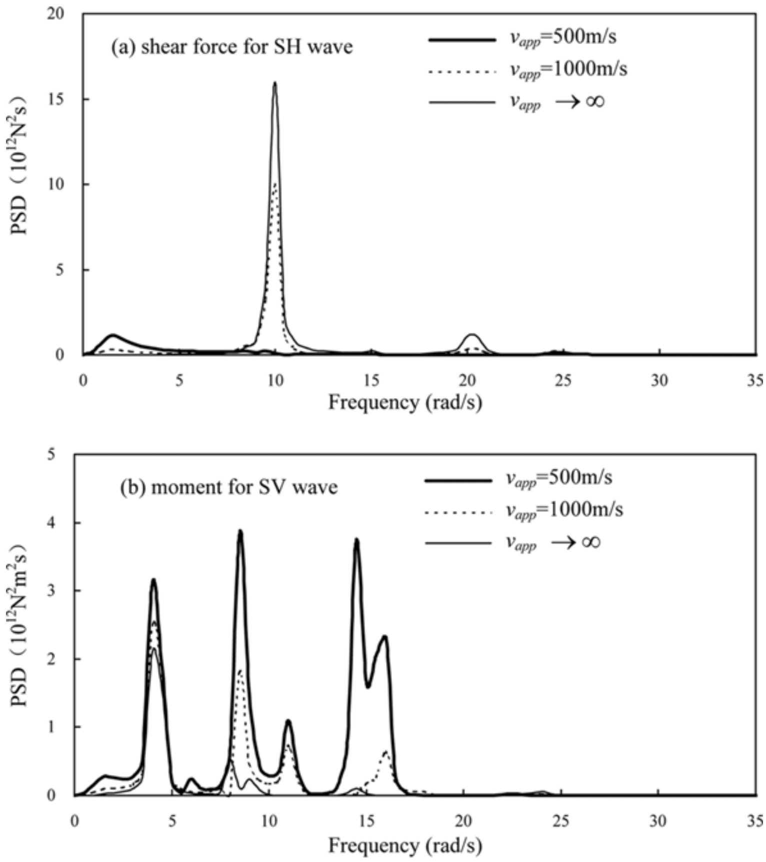

Fig. 8 Power spectral density at support 2 for the shear force due to an SH wave and the moment caused by an SV wave

5. Conclusions

In the present paper, the seismic random responses due to the wave passage effect have been extensively numerically investigated, based on PEM. The results have shown that the wave passage effect has a significant influence on structural responses. In particular, the internal force responses have been shown to vary significantly with the apparent wave velocity, especially when the wave velocity is rather low or the span is very long. Such variations do not vary monotonically, especially for flexible structures. The quasi-static and the dynamic components both depend heavily on the seismic wave velocity and the natural frequencies of the structure. A simple example has shown that the dynamic component has a very significant effect on the dynamic responses of structures with low natural frequencies, whereas the quasi-static component dominates for structures with higher frequencies unless the wave speed is also high.

For complex structures, it is usually difficult to judge the main participating natural frequencies that will affect the structural responses severely. In addition, the seismic wave velocity may vary significantly with different circumstances, and the results presented for a suspension bridge show that the response varies considerably with wave speed. Therefore unless relatively precise data is available, it may be advisable for designers to select a range of possible velocities and to base their design on the most conservative result thus obtained. Because of the high speed of PEM, this is not unduly time consuming, e.g. the computations for the suspension bridge of Example 2 took less than one minute per apparent wave speed selected when using a Pentium-3 personal computer with main frequency 900 MHz and a memory of 256 M.

Acknowledgements

This work has been supported by NSFC (No. 10472023). The work described in this paper was also supported by a grant from City University of Hong Kong (Project No. 7001591). The authors are grateful for the support from City University of Hong Kong in the funding of their cooperation. The third author was on leave of absence from Cardiff University when this paper was written and has since returned there.

References

Berrah, M. and Kausel, E. (1992), "Response spectrum analysis of structures subjected to spatially varying motions", *Earthq. Eng. Struct. Dyn.*, **21**(6), 461-470.

Clough, R.W. and Penzien, J. (1993), *Dynamics of Structures*, McGraw-Hill, New York.

Davenport, A.G. (1961), "The application of statistical concepts to the wind loading of structures", *Proc. Inst. Civil Eng.*, London, **19**, (August), 449-472.

Dumanoglu, A.A. and Soyluk, K. (2003), "A stochastic analysis of long span structures subjected to spatially varying ground motions including the site-response effect", *Eng. Struct.*, **25**(10), 1301-1310.

Hawwari, A.R. (1992), "Suspension bridge response to spatially varying ground motion", PhD thesis, Michigan State Univ. East Lansing, Mich.

Harichandran, R.S. and Vanmarcke, E.H. (1986), "Stochastic variation of earthquake ground motion in space and time", *J. Eng. Mech.*, ASCE, **112**(2), 154-175.

Heredia-Zavoni, E. and Vanmarcke, E.H. (1994), "Seismic random vibration analysis of multi-support structural systems", *J. Eng. Mech.*, ASCE, **120**(5), 1107-1128.

Kiureghian, A.D. and Neuenhofer, A. (1992), "Response spectrum method for multi-support seismic excitations", *Earthq. Eng. Struct. Dyn.*, **21**(8), 713-740.

Kiureghian, A.D. and Neuenhofer, A. (1995), "A discussion on seismic random vibration analysis of multi-support structural systems", *J. Eng. Mech.*, ASCE, **121**(9), 1037.

Kiureghian, A.D. (1996), "A coherency model for spatially varying ground motions", *Earthq. Eng. Struct. Dyn.*, **25**(1), 99-111.

Lee, M.C. and Penzien, J. (1983), "Stochastic analysis of structures and piping systems subjected to stationary multiple support excitations", *Earthq. Eng. Struct. Dyn.*, **11**(1), 91-110.

Lin, J.H. (1992), "A fast CQC algorithm of PSD matrices for random seismic responses", *Comput. Struct.*, **44**(3), 683-687.

Lin, J.H., Li, J.J., Zhang, W.S. and Williams, F.W. (1997), "Non-stationary random seismic responses of multi-support structures in evolutionary inhomogeneous random fields", *Earthq. Eng. Struct. Dyn.*, **26**(1), 135-145.

Lin, J.H., Zhang, Y.H., Li, Q.S. and Williams, F.W. (2004), "Seismic spatial effects for long-span bridges, using the pseudo excitation method", *Eng. Struct.*, **26**(9), 1207-1216.

Lin, Y.K., Zhang, R. and Yong, Y. (1990), "Multiply supported pipeline under seismic wave excitations", *J. Eng. Mech.*, ASCE, **116**(5), 1094-1108.

Loh, C.H. and Yeh, Y.T. (1988), "Spatial variation and stochastic modeling of seismic differential ground movement", *Earthq. Eng. Struct. Dyn.*, **16**(5), 583-596.

Tubino, F., Carassale, L. and Solari, G. (2003), "Seismic response of multi-supported structures by proper orthogonal decomposition", *Earthq. Eng. Struct. Dyn.*, **32**(11), 1639-1654.

Werner, S.D., Lee, L.C., Wong, H.L. and Trifunac, M.D. (1979), "Structural response to traveling seismic waves", *J. Struct. Div.,* ASCE, **105**(12), 2547-2564.

Yamamura, N. and Tanaka, H. (1990), "Response analysis of flexible MDF systems for multiple-support seismic excitations", *Earthq. Eng. Struct. Dyn.*, **19**(3), 345-357.